

1
2
3
4
5
6
7
8
9
10
11
12
13
14
15
16
17
18
19
20
21

Matrix porosity is associated with *Staphylococcus aureus* biofilm survival during prosthetic joint infection

Mohini Bhattacharya¹, Tyler D. Scherr², Jessica Lister³, Tammy Kielian², Alexander R. Horswill^{1,4*}

¹Department of Immunology and Microbiology, University of Colorado School of Medicine, Aurora, CO, USA

²Department of Pathology, Microbiology, and Immunology, University of Nebraska Medical Center, Omaha, NE, USA

³Department of Microbiology, University of Iowa, Iowa City, Iowa, USA

⁴Department of Veterans Affairs, Eastern Colorado Health Care System, Aurora, CO, USA

*Corresponding Author

Alexander R. Horswill

Department of Immunology and Microbiology, University of Colorado, Anschutz Medical Campus

12800 East 19th Avenue Aurora, CO, USA.

Phone: (303) 724-4224, Fax: (303) 724-4226,

E-mail: alexander.horswill@cuanschutz.edu

Running title: Matrix proteins protect MRSA biofilms from macrophages

22 **Abstract.** Biofilms are a cause of chronic, non-healing infections. *Staphylococcus*
23 *aureus* is a proficient biofilm forming pathogen commonly isolated from prosthetic joint
24 infections that develop following primary arthroplasty. Extracellular adhesion protein
25 (Eap), previously characterized in planktonic or non-biofilm populations as being an
26 adhesin and immune evasion factor, was recently identified in the exoproteome of *S.*
27 *aureus* biofilms. This work demonstrates that Eap and its two functionally orphaned
28 homologs EapH1 and EapH2, contribute to biofilm structure and prevent macrophage
29 invasion and phagocytosis into these communities. Biofilms unable to express Eap
30 proteins demonstrated increased porosity and reduced biomass. We describe a role for
31 Eap proteins *in vivo* using a mouse model of *S. aureus* prosthetic joint infection. Results
32 suggest that the protection conferred to biofilms by Eap proteins is a function of biofilm
33 structural stability that interferes with the leukocyte response to biofilm-associated
34 bacteria.

35

36 **Keywords.** MRSA, biofilm, matrix, immune clearance

37 Introduction

38 The Gram-positive pathogen, *Staphylococcus aureus*, has been the causative
39 agent of >119,000 bloodstream infections in the United States, with nearly 20,000 deaths
40 caused by methicillin resistant S. aureus (MRSA) [1], [2]. Recent studies show that while
41 measures to control hospital-associated bacterial transmission have reduced the
42 occurrence of serious *S. aureus* infections, this success has been slowing [2].
43 Approximately 1-3% of total hip and knee arthroplasties continue to be complicated by
44 infection, resulting in longer hospital stays, higher occurrence of revision surgeries, and
45 decreased 5- year survival rates [3], [4]. Along with the acquisition of resistance to many
46 currently prescribed antibiotics, the ability of *S. aureus* to form biofilms during chronic
47 infections has made this pathogen a substantial cause of concern with approximately 20%
48 of surgical site infections reported to be associated with *S. aureus* [4], [5]. Biofilm-
49 associated bacteria can tolerate up to 1,000 times the antibiotic concentrations that are
50 found to be effective against planktonic or non-biofilm forms of the same strain [6], [7].
51 Furthermore, biofilms are generally recognized as a distinct lifestyle with uniquely
52 attributable virulence mechanisms [8], [9], [10], [11]. Bacteria communicate within biofilms
53 via quorum sensing molecules that allow for the development of shared, public goods
54 [12]. A consequence of this is the formation of a protective matrix surrounding the biofilm,
55 consisting of one or more components, including proteins, DNA and/or polysaccharides
56 [13], [14]. Since biofilms are formed under nutritional or environmental stresses, this often
57 allows the pathogen to evade host antimicrobial responses until conditions that are
58 favorable for planktonic growth become available [15]. When this occurs, biofilm-
59 associated bacteria disperse from the community and often cause disseminated
60 infections including, but not limited to, serious bloodstream-associated conditions [15],
61 [16], [17]. Therefore, it is imperative that biofilm-associated phenotypes are considered in
62 the prevention of persistent *S. aureus* infections [18].

63 One of the major secreted and surface-associated proteins found in the *S. aureus*
64 biofilm matrix is extracellular adherence protein (Eap), which is reported to ubiquitously
65 bind to numerous host proteins as well as bacterial and host DNA [19]. Eap is primarily
66 secreted from *S. aureus* but is also described as being able to subsequently bind to the
67 bacterial surface via the activity of a neutral phosphatase and other, yet uncharacterized

68 factors [20]. Previous studies with planktonic bacteria attribute important anti-
69 inflammatory and anti-angiogenic properties to Eap during *S. aureus* endovascular
70 infection [21]. While this protein has been demonstrated to contribute to biofilm formation
71 under conditions of stress, including iron starvation and the presence of serum, the role
72 that Eap could play as a virulence factor during biofilm growth, is currently understudied
73 [22], [23]. *S. aureus* also expresses two functional orphans of Eap, EapH1 and EapH2,
74 recently reported to protect the bacterium against neutrophil-derived proteases [24], [25].

75 Macrophages have been established as being crucial for an effective immune
76 response to *S. aureus* in wounds and foreign body-associated infections [26], [27], [28],
77 [29]. Here we show that the expression of the three Eap proteins (Eap, EapH1 and
78 EapH2) prevents macrophages from invading and phagocytosing *S. aureus* biofilm
79 bacteria. These phenotypes are specific to macrophages since neutrophils were relatively
80 unaffected by the presence of Eap. Additionally, using an established murine model of
81 prosthetic joint infection we show that the inability to express Eap causes a significant
82 reduction in bacterial burdens in the joint as well as surrounding tissue [26], [30]. Together
83 these data provide evidence for the role of Eap as a biofilm structural protein that
84 promotes *S. aureus* orthopedic infections.

85 **Results**

86 **Eap proteins contribute to biofilm biomass and structure**

87 To understand if Eap plays a role in biofilm development, we compared the gross biofilm
88 biomass of the most commonly isolated *S. aureus* lineage, USA300 (hereafter referred to
89 as WT) to an isogenic mutant lacking *eap* as well as its two functionally orphaned
90 homologs, *eapH1* and *eapH2* (hereafter Δeap) using an established crystal violet-based
91 assay [31]. Biomass comparisons of biofilms from both strains grown for 24 hours showed
92 that Δeap bacteria have a significant loss of biomass compared to WT biofilms (**Figure**
93 **1A**). The immunomodulatory protein IsaB is another DNA binding protein that is
94 abundantly expressed as part of the biofilm exoproteome of common clinical strains of *S.*
95 *aureus* [32], [33]. We therefore generated a mutant of the *isaB* gene in the Δeap strain
96 background. Bacteria lacking IsaB in addition to the three Eap proteins, formed biofilms
97 with biomass comparable to Δeap bacteria (**Figure 1A**). These results indicate that while
98 the 3 Eap proteins are important for biofilm structure, the immunomodulatory surface

99 protein IsaB does not significantly contribute to *in vitro* biofilm formation under these
100 conditions. Confocal microscopy was used to further investigate the differences in gross
101 biomass of 24-hour biofilms observed with crystal violet assays. 3D images indicated that
102 when compared to WT biofilms, Δeap and $\Delta eap\Delta isaB$ biofilms showed a loss of structure
103 and thickness (**Figure 1B**). Quantification of biofilm biomass from confocal microscopy
104 confirmed that Δeap biofilms have a significant loss of thickness compared to WT biofilms
105 and that there was no further decreases in the isogenic $\Delta eap\Delta isaB$ strain (**Figure 1C**).
106 Collectively these data indicate that Eap proteins contribute to the gross biofilm biomass
107 and that these proteins may also play a specific role in the overall structure of *S. aureus*
108 biofilms.

109 **Eap proteins contribute to the porosity of *S. aureus* biofilms.** To further investigate
110 a role for Eap proteins in providing a specific structural advantage to *S. aureus* biofilms,
111 we tested for differences in porosity when WT biofilms were compared to those formed
112 by the isogenic mutants, Δeap and $\Delta eap\Delta isaB$. We utilized 3 sizes of fluorescein
113 isothiocyanate (FITC) labelled dextran (10k, 70k and 150k) and allowed biofilms to grow
114 on 0.45 μ m membranes before measuring the levels of each FITC-dextran that could
115 penetrate through biofilms formed by each strain using previously established methods
116 [33]. While there were no differences between strains in the levels of 10k FITC-labelled
117 dextran that could penetrate through biofilms (**Figure 2A**), we observed a significant
118 increase in the porosity of mutants lacking Eap proteins compared to WT, when biofilms
119 were incubated with 70 (**Figure 2B**) and 150k FITC-labelled dextran (**Figure 2C**).
120 Additionally, we used 24-hour biofilms grown in 6-channel ibidi flow cells to image the
121 entry and retention of various sizes of FITC-dextran as described above. Confocal images
122 of biofilms incubated with each FITC-dextran for 1 hour, followed by 3 washes in saline
123 revealed, that the levels of 70k and 150k (but not 10k) FITC-labelled dextran that could
124 penetrate and be retained in Δeap and $\Delta eap\Delta isaB$ biofilms was higher than the WT control
125 (**Figure 2D**). These data together indicate that Eap proteins reduce the overall porosity
126 of *S. aureus* biofilms, and that the absence of these 3 proteins increases access to the
127 biofilm.

128

129 **Eap proteins reduce macrophage invasion and phagocytosis of *S. aureus* biofilms.**

130 Previous reports describe a role for Eap in protecting planktonic *S. aureus* against human
131 neutrophils. While Eap, EapH1 and EapH2 were shown to inhibit neutrophil proteases,
132 Eap was shown to bind to neutrophil DNA and interfere with neutrophil extracellular trap
133 (NET) formation [24], [34]. Since we found that *S. aureus* biofilms lacking Eap proteins
134 were significantly more porous with reduced biomass, we examined whether these
135 differences would affect the ability of biofilms to evade phagocytosis by innate immune
136 cells [27], [35]. Macrophages and neutrophils are crucial in the innate immune response
137 to infection [36], [37], [38]. We therefore incubated mature biofilms with either primary
138 murine bone marrow-derived macrophages or neutrophils for 4-6 h to quantify the number
139 of leukocytes that could penetrate and phagocytose either WT or Δeap biofilms. Since no
140 significant differences were observed between the Δeap and $\Delta eap\Delta isaB$ biofilms in earlier
141 studies, WT was compared with the Δeap strain for these assays. Macrophage invasion
142 into Δeap biofilms was significantly increased compared to WT, as reflected by both
143 visualization (**Figure 3A, B**) and quantification (**Figure 3C**). Additionally, quantification of
144 macrophages containing bacteria were also significantly higher in Δeap mutant biofilms
145 compared to WT (**Figure 3D**) [27]. Lastly, the total number of observable macrophages
146 associated with Δeap mutant biofilms was significantly higher compared to WT indicating
147 that there were more intact macrophages that are phagocytosing bacteria in Δeap biofilms
148 (**Figure 3E**). These results together demonstrate that Eap proteins reduce the invasion
149 and phagocytosis of *S. aureus* biofilms by macrophages.

150 When similar experiments were performed with primary murine neutrophils,
151 although larger numbers of neutrophils could be observed invading Δeap biofilms
152 compared to WT (**Figure S1A and B**) this did not reach statistical significance (**Figure**
153 **S1C**). Furthermore, there were no differences in the numbers of neutrophils observed
154 phagocytosing biofilm (**Figure S1D**) or total number of neutrophils present (**Figure S1E**),
155 between WT and Δeap biofilms. Collectively, these results indicate a larger role for Eap
156 in preventing phagocytosis and clearance of biofilms by macrophages, in comparison to
157 neutrophils.

158 **Eap proteins contribute to *S. aureus* prosthetic joint infection.** Since biofilms lacking
159 Eap proteins were more susceptible to invasion and phagocytosis by macrophages *in*

160 *vitro* and exhibited less structural organization, we next examined whether these
161 phenotypes would translate to altered biofilm survival *in vivo*. A previously established
162 mouse model of prosthetic joint infection was used to compare the ability of Δeap to form
163 biofilm compared to WT bacteria [39], [40]. Three time points were selected to reflect
164 planktonic growth (day 3), transition to biofilm formation (day 7), and chronicity (day 14)
165 based on recalcitrance to systemic antibiotics [29]. A larger number of animals was
166 analyzed at day 7 since this represents the transition period to biofilm growth and was
167 considered the best interval to interrogate potential phenotypes given the biofilm
168 structural defects observed with Δeap *in vitro*. Bacterial burden was significantly reduced
169 in the tissue surrounding the infected joint with Δeap bacteria at days 7 and 14 post-
170 infection, which extended to the joint at day 7 with a trending decrease at day 14 (**Figure**
171 **4A-B**). Titers in the femur were also lower at days 7 and 14 with Δeap , although this did
172 not reach statistical significance, and no differences were observed on the implant
173 (**Figure 4C-D**). Previous work has described the role of granulocytic myeloid-derived
174 suppressor cells (G-MDSCs) in promoting *S. aureus* biofilm survival by their ability to
175 inhibit macrophage proinflammatory activity, neutrophil antimicrobial activity, and T cell
176 activation [26], [39], [41]. Therefore, flow cytometry was performed on infected tissue
177 samples to quantify G-MDSC infiltrates between WT and Δeap infected mice [42].
178 Although the overall number of CD45⁺ leukocytes trended higher in WT infected mice
179 compared to those infected with Δeap bacteria (**Figure S2A**), G-MDSC infiltrates
180 (CD45⁺Ly6G⁺Ly6C⁺) were similar between the groups (**Figure S2B**). Since neutrophils
181 are also recruited to infected tissues, we measured the number of neutrophils
182 (CD45⁺Ly6G⁺Ly6C⁻) in these animals (**Figure S2C**). While Δeap infected mice had lower
183 neutrophil numbers compared to WT at day 7, these differences were not statistically
184 significant at day 14. Altogether these data suggest that Eap proteins play specific roles
185 in promoting *S. aureus* survival during biofilm-associated infection *in vivo*. Furthermore,
186 while G-MDSC and neutrophil responses were generally comparable between WT and
187 Δeap infected conditions, the consequence of this response to bacterial survival is likely
188 altered as a function of Eap expression based on our *in vitro* findings.

189

190

191 **Discussion**

192 This work provides evidence that Eap proteins are important to *S. aureus* biofilm
193 structure and can influence the host response to infection. We demonstrate that Eap
194 proteins increase the thickness (**Figure 1**) and reduce the porosity (**Figure 2**) of *S.*
195 *aureus* biofilms, and this affects macrophage functions (**Figure 3**). Although to a smaller
196 extent these proteins also confer an advantage to biofilms that are exposed to neutrophils
197 (**Figure S1**). *In vivo*, while Eap proteins do not seem to alter the overall innate immune
198 response to *S. aureus* biofilm infection, bacterial survival was significantly reduced with
199 Δeap compared to WT bacteria (**Figure 4**). When taken together with our *in vitro* findings,
200 this suggests that Eap proteins may serve to prevent bacterial clearance by phagocytes
201 *in vivo* (**Figure 5**). It is unlikely that these phenotypes are due solely to the increased
202 access afforded to phagocytic cells by virtue of a reduction in biofilm thickness and
203 porosity.

204 Previous reports have shown that Eap proteins are anti-inflammatory and
205 immunomodulatory, with anti-protease activity specifically against human neutrophils.
206 Eap is also known to prevent the degradation of phenol soluble modulins (PSMs)
207 by neutrophil-derived proteases [43]. PSMs can lyse neutrophils and are released during
208 the transition of biofilms to planktonic growth, making them an important virulence factor
209 during infection [44]. PSMs are also reported to form amyloid fibers that can stabilize
210 biofilm structure [45]. Whether PSMs contribute to Eap-associated tolerance of
211 neutrophils warrants further investigation. Similarly, while studies report a role for Eap in
212 binding to DNA and blocking NET formation, *S. aureus* biofilms are documented to induce
213 NETosis in a leukocidin-dependent manner and to utilize a nuclease to degrade the DNA
214 released from neutrophils [34], [35], [46]. Since experiments with Eap were performed
215 with purified protein and chemically induced NETs, analyzing the effect of Eap proteins
216 on NETs released from biofilms would provide more information on the role of Eap
217 proteins during neutrophil ET release [34]. Additionally, it has been demonstrated that
218 once Eap binds DNA it does not cleave it [34]. It is therefore possible that Eap-bound host
219 DNA can act as an immune evasion strategy *in vivo*, allowing *S. aureus* to appear as a
220 'self' molecule to the immune system, although this remains speculative.

221

222 Here we demonstrate that Eap proteins can provide *S. aureus* with some degree of
223 protection against macrophages *in vitro*. Eap expressed by planktonic bacteria interacts
224 with peripheral blood mononuclear cells presumably via the intercellular adhesion
225 molecule 1 (ICAM-1) to induce proinflammatory cytokine production (IL-6, TNF- α) [47].
226 Biofilms bias macrophage towards an anti-inflammatory phenotype (arginase-1, IL-4, IL-
227 10) that is compounded by the action of immune suppressive G-MDSCs known to impair
228 T cell activation [27], [48]. These biofilm-specific mechanisms of macrophage subversion
229 may therefore neutralize any proinflammatory signals generated as a function of Eap.
230 Conversely, a number of reports provide evidence that Eap impairs neutrophil and T cell
231 recruitment as well as T cell activation. These functions were attributed to higher
232 concentrations of Eap such as those that would be produced by bacterial biofilms [21],
233 [49], [50]. It is therefore likely that the anti-inflammatory properties of Eap are more
234 relevant during biofilm infections, whereas proinflammatory processes are associated
235 with survival of planktonic populations.

236 Lastly, in addition to DNA, Eap proteins have been documented to promiscuously
237 bind multiple host-associated ligands including fibrinogen and collagen. Synovial fluid is
238 an ultrafiltrate of blood plasma that encases joints and periprosthetic implants [51], [52],
239 [53]. Whether Eap promiscuously binds to components of synovial fluid is currently
240 unknown. This viscous fluid is known to harbor *S. aureus* aggregate biofilms reported to
241 bind fibrinogen via its two sortase anchored fibronectin binding proteins FnbpA and B
242 [54]. The properties of these biofilms are distinct from their surface-associated
243 counterparts and can be formed by subpopulations of detached biofilm bacteria [55]. It is
244 therefore plausible that the Eap proteins, FnbpA and FnbpB could contribute to biofilm
245 survival at different phases of the infection lifecycle and require the additional activities of
246 dispersion cues including PSMs to evade the immune response during prosthetic joint
247 infection. Altogether this work builds on previous studies and adds to our knowledge of
248 the innate immune response to *S. aureus* biofilm infections. **Figure 5** summarizes our
249 findings and hypotheses based on current and previous work to depict how Eap proteins
250 may be playing a multifactorial role during *S. aureus* biofilm-associated prosthetic joint

251 infection, with potential new avenues of investigation to better understand the complex
252 dynamics that make *S. aureus* a successful biofilm pathogen.

253 **Resource availability**

254 Lead Contact

255 Further inquiries and information on reagents and resources should be directed to (and
256 will be fulfilled by) the lead contact, Alexander R. Horswill.

257 (alexander.horswill@cuanschutz.edu)

258 Materials availability

259 Reagents and materials used or generated in this study can be made available upon
260 request from the lead contact.

261 Data availability

262 Data reported in this manuscript will be made available by the lead contact upon request.

263

264 **Author Contributions.** Conceptualization, M.B., T.D.S., J.L., T. K., A.R.H.; Methodology,
265 M.B., T.D.S., T. K., A.R.H.; ; Investigation, M.B., T.D.S., J.L.; ; Writing- Original Draft, M.B.,
266 Writing- Review and Editing, M.B., T.K., A.R.H.; Funding Acquisition, T.K, and A.R.H.;
267 Supervision, T.K., A.R.H.

268

269 **Acknowledgments.** The authors would like to thank members of the Horswill and Kielian
270 groups for their critical evaluation of the data in this manuscript. This work was funded by
271 the NIH/NIAID grant(s) AI083211 to A.R.H. and T.K., and VA Merit Award BX002711 to
272 A.R.H

273 **Declaration of interests.** The authors declare no competing interests.

274

275 **Supplemental Information**

276 Document S1. Figures S1, S2

277

278 **Materials and Methods.**

279 **Bacterial strains and growth conditions.** Unless otherwise indicated all experiments
280 were performed in the USA300 clinical strain background. Bacterial cultures were grown
281 in tryptic soy broth (TSB) at 37°C with shaking (200RPM).

282

283 **Construction of *S. aureus* bacterial mutants.** Chromosomal deletions of the three *Eap*
284 encoding genes (*eap*, *eapH1* and *eapH2*) were performed using previously established
285 methods [33]. Briefly, the temperature sensitive pJB38 plasmid was used to introduce
286 DNA fragments (~1kb) flanking the target region of interest. Flanking DNA was amplified
287 (Phusion high fidelity polymerase, NE Biolabs) using gene specific primers, products were
288 digested with restriction enzymes (Table 2) and purified (Qiagen PCR purification).
289 Following triple ligation into pJB38, the plasmid was electroporated into *E. coli* DC10b
290 and selected for on Luria Bertani agar plates containing 100µg/mL ampicillin. Following
291 confirmation from single colonies, plasmid was purified, PCR used for confirmation with
292 construction and sequencing primers performed and plasmid was electroporated into *S.*
293 *aureus*. Positive clones were selected on tryptic soy agar (TSA) containing 10µg/mL
294 chloramphenicol and homologous recombination performed at 42 degrees for 24 hours.
295 Following overnight incubation in TSA-Cam and a series of subcultures in TSB at 30
296 degrees, counterselection was performed on 200 ng/ml anhydrotetracycline (30 degrees/
297 overnight). Loss of plasmid was indicated by growth on TSA but not TSA-Cam and
298 presence of desired mutations were verified using PCR with chromosomal primers that
299 were outside the region of mutation.

300

301 ***In vitro* 24- hour biofilm growth.** All *in vitro* biofilms used for biomass and matrix porosity
302 measurements were grown in TSB containing 0.4% glucose as previously published,
303 unless otherwise indicated [33], [56]. Bacterial cultures were grown overnight (16- 18
304 hours) in TSB at 37°C with shaking (200RPM). The next day, bacteria were sub cultured
305 (1:100) in fresh TSB for 2-3 hours and brought to exponential phase corresponding to an
306 optical density (OD) at 600nm of 0.5- 0.7 as previously described. Cultures were then
307 centrifuged at 3900RPM for 2 minutes, washed once with phosphate buffered saline

308 (PBS), centrifuged and re-suspended in TSB containing 0.4% glucose for biofilm growth
309 measurements.

310

311 **Biofilm biomass measurements using crystal violet staining.** Cultures were prepared
312 in TSB containing 0.4% glucose as described above. Bacteria were seeded into 96- well
313 microtiter plates (Costar, 200 μ L per well) and incubated overnight at 37°C in a humidified
314 chamber for 24 hours. Biofilms were washed with double distilled water (dd water) and
315 incubated with 0.1% crystal violet for 30 minutes at room temperature. Crystal violet was
316 drained, and plate was washed in dd water 3 times followed by addition of 33% acetic
317 acid to the wells. After a 30-minute incubation, solubilized biofilms were pipetted into a
318 new 96 well plate and O.D was measured at 575nm. Measurements were made in
319 comparison to well containing PBS.

320

321 ***In vitro* biofilms for confocal imaging.** Cultures were prepared in TSB containing 0.4%
322 glucose as described above. Bacteria were seeded into 8-well ibidi μ -slides (ibidi,
323 Cat.No:80826) and incubated for 24 hours at 37°C in a humidified chamber. Spent media
324 was removed, biofilms were washed with PBS and stained with 10 μ g/mL Hoechst Blue
325 33342 stain (Thermo Fisher, Cat.No: H3570) for 30 minutes for confocal imaging. Biofilms
326 were then washed again with PBS and fixed with 10% formalin. Biofilms were visualized
327 using the Olympus FV1000 confocal laser scanning microscope using the Z-stack feature
328 to collect 3D images spanning the thickness of the biofilm. All experiments were
329 performed with 2 technical duplicate biofilms per strain for a total n= 4 (n=8 biofilm
330 technical replicates per strain). 3 images were taken per technical biofilm replicate (n=24
331 images per strain).

332

333 **Measuring porosity of *in vitro* biofilms.** 24- hour biofilms of WT or respective isogenic
334 mutants were grown as described above in 96 well plates containing 0.45 μ m PVDF
335 membranes as previously described [33]. Briefly, biofilms grown in 96-well plates without
336 a membrane were used as a negative control. Following 24-hour growth, control biofilm
337 biomass was measured using the crystal violet assay described above. Media was
338 removed from filter plates and replaced with 100 μ L MES (2-(N-morpholino)ethane

339 sulfonic acid) (MES) buffer containing 1mg/mL FITC-isocyanide-dextran (with dextran at
340 a molecular weight of either 4K, 10K, 70K, or 150K). These experiments were performed
341 using a negative control consisting of biofilms resuspended in buffer lacking FITC-
342 dextran. Filter plates were centrifuged for 45 seconds at 20g, flow through collected and
343 relative levels of fluorescence measured with excitation and emission wavelengths of
344 470 nm and 523 nm respectively. Values were plotted in comparison to the media-only
345 control as a measure of maximum fluorescence. For microscopy, bacteria were grown as
346 described above and seeded into 8-well ibidi μ -slides (ibidi, Cat.No:80826). Biofilms were
347 washed in PBS and resuspended in 1mg/mL FITC-isocyanide-dextran of various sizes as
348 described above, for 1 hour. 3D images were taken using the Olympus FV1000 system.

349

350 ***S. aureus* biofilm-leukocyte co-culture experiments.** Confocal microscopy
351 experiments depicting the interaction of macrophages or neutrophils with *S. aureus*
352 biofilms were performed as previously published [27]. Briefly, green fluorescent protein
353 (GFP) labelled bacteria were grown to exponential phase as described above and seeded
354 into chamber slides coated with human plasma. Biofilms were allowed to grow for 4 days
355 at 37°C and incubated with Cell Tracker Blue labelled bone marrow-derived macrophages
356 or thioglycolate-elicited neutrophils from C57BL/6 mice for 4-6 h using a Zeiss laser
357 scanning confocal microscope (LSM 710 META; Carl Zeiss). 3D images of biofilms were
358 collected using Xen 2007 software (Carl Zeiss) as previously described [27]. The number
359 of leukocytes invading and phagocytosing biofilms was quantified by measuring the
360 distance of immune cells from the biofilm base (invasion) and number of leukocytes with
361 intracellular bacteria in each field of view using orthogonal images.

362

363 **Mouse prosthetic joint infection model.** *S. aureus* biofilm infection was studied *in vivo*
364 using an established model of implant-associated prosthetic joint infection. Briefly, 8–10-
365 week-old male and female C57BL/6 mice (n=5-10 mice/time point/strain) were used to
366 introduce an implant into the intramedullary canal of the femur as previously described
367 [26], [30], [39], [42]. Approximately 10^3 of WT or Δ lep bacteria were inoculated at the
368 implant tip and animals were administered buprenorphine slow release (SR) after surgery
369 for pain relief. Animals were euthanized at days 3, 7, and 14 post-infection to collect tissue

370 and implant samples as previously described [42]. Tissue homogenates and sonicated
371 implants were plated on TSA containing 5% sheep blood to quantify total colony forming
372 units (cfu) per gram of tissue or per mL diluent for implants. The soft tissue surrounding
373 the knee was collected to quantify G-MDSC and PMN infiltrates by flow cytometry using
374 antibodies for CD45, Ly6G, and Ly6C as previously described [42].

375

- 376 [1] “Deadly Staph Infections Still Threaten the U.S. | CDC Online Newsroom | CDC.”
377 Accessed: Dec. 20, 2022. [Online]. Available:
378 <https://www.cdc.gov/media/releases/2019/p0305-deadly-staph-infections.html>
- 379 [2] “Current HAI Progress Report | HAI | CDC.” Accessed: Jun. 14, 2023. [Online]. Available:
380 <https://www.cdc.gov/hai/data/portal/progress-report.html>
- 381 [3] A. J. Tande and R. Patel, “Prosthetic joint infection,” *Clin Microbiol Rev*, vol. 27, no. 2, pp.
382 302–345, 2014, doi: 10.1128/CMR.00111-13.
- 383 [4] M. de Buys, K. Moodley, J. N. Cakic, and J. R. T. Pietrzak, “*Staphylococcus aureus*
384 colonization and periprosthetic joint infection in patients undergoing elective total joint
385 arthroplasty: a narrative review,” *EFORT Open Rev*, vol. 8, no. 9, p. 680, Sep. 2023, doi:
386 10.1530/EOR-23-0031.
- 387 [5] M. Saadatian-Elahi, R. Teyssou, and P. Vanhems, “*Staphylococcus aureus*, the major
388 pathogen in orthopaedic and cardiac surgical site infections: a literature review,” *Int J*
389 *Surg*, vol. 6, no. 3, pp. 238–245, 2008, doi: 10.1016/J.IJSU.2007.05.001.
- 390 [6] H. Ceri, M. E. Olson, C. Stremick, R. R. Read, D. Morck, and A. Buret, “The Calgary Biofilm
391 Device: new technology for rapid determination of antibiotic susceptibilities of bacterial
392 biofilms,” *J Clin Microbiol*, vol. 37, no. 6, pp. 1771–1776, 1999, doi:
393 10.1128/JCM.37.6.1771-1776.1999.
- 394 [7] R. P. Howlin, M. J. Brayford, J. S. Webb, J. J. Cooper, S. S. Aiken, and P. Stoodley,
395 “Antibiotic-loaded synthetic calcium sulfate beads for prevention of bacterial
396 colonization and biofilm formation in periprosthetic infections.,” *Antimicrob Agents*
397 *Chemother*, vol. 59, no. 1, pp. 111–20, Jan. 2015, doi: 10.1128/AAC.03676-14.
- 398 [8] C. Guilhen *et al.*, “Transcriptional profiling of *Klebsiella pneumoniae* defines signatures
399 for planktonic, sessile and biofilm-dispersed cells,” *BMC Genomics*, vol. 17, no. 1, pp. 1–
400 15, Mar. 2016, doi: 10.1186/s12864-016-2557-x.
- 401 [9] K. Daw, A. S. Baghdayan, S. Awasthi, and N. Shankar, “Biofilm and planktonic
402 *Enterococcus faecalis* elicit different responses from host phagocytes *in vitro*,” *FEMS*
403 *Immunol Med Microbiol*, vol. 65, no. 2, pp. 270–282, Jul. 2012, doi: 10.1111/j.1574-
404 695X.2012.00944.x.
- 405 [10] A. Resch, R. Rosenstein, C. Nerz, and F. Götz, “Differential gene expression profiling of
406 *Staphylococcus aureus* cultivated under biofilm and planktonic conditions.,” *Appl Environ*
407 *Microbiol*, vol. 71, no. 5, pp. 2663–2676, 2005, doi: 10.1128/AEM.71.5.2663.
- 408 [11] M. Bhattacharya and A. R. Horswill, “The role of human extracellular matrix proteins in
409 defining *Staphylococcus aureus* biofilm infections,” *FEMS Microbiol Rev*, vol. 48, p. 2,
410 2024, doi: 10.1093/femsre/fuae002.
- 411 [12] S. Mukherjee and B. L. Bassler, “Bacterial quorum sensing in complex and dynamically
412 changing environments,” *Nature Reviews in Microbiology*, vol. 17, 2019, doi:
413 10.1038/s41579-019-0186-5.
- 414 [13] J. W. Costerton *et al.*, “Bacterial Biofilms in Nature and Disease,” *Annu Rev Microbiol*, vol.
415 41, no. 1, pp. 435–464, Oct. 1987, doi: 10.1146/annurev.mi.41.100187.002251.
- 416 [14] H. C. Flemming *et al.*, “The biofilm matrix: multitasking in a shared space,” *Nat Rev*
417 *Microbiol*, vol. 21, no. 2, pp. 70–86, Feb. 2023, doi: 10.1038/S41579-022-00791-0.

- 418 [15] L. Hall-Stoodley *et al.*, “Towards diagnostic guidelines for biofilm-associated infections.,”
419 *FEMS Immunol Med Microbiol*, vol. 65, no. 2, pp. 127–45, Jul. 2012, doi: 10.1111/j.1574-
420 695X.2012.00968.x.
- 421 [16] C. A. Fux, J. W. Costerton, P. S. Stewart, and P. Stoodley, “Survival strategies of infectious
422 biofilms.,” *Trends Microbiol*, vol. 13, no. 1, pp. 34–40, Jan. 2005, doi:
423 10.1016/j.tim.2004.11.010.
- 424 [17] N. Høiby, T. Bjarnsholt, M. Givskov, S. Molin, and O. Ciofu, “Antibiotic resistance of
425 bacterial biofilms.,” *Int J Antimicrob Agents*, vol. 35, no. 4, pp. 322–32, Apr. 2010, doi:
426 10.1016/j.ijantimicag.2009.12.011.
- 427 [18] M. Bhattacharya, D. J. Wozniak, P. Stoodley, and L. Hall-Stoodley, “Prevention and
428 treatment of *Staphylococcus aureus* biofilms,” *Expert Rev Anti Infect Ther*, vol. 13, no. 12,
429 2015.
- 430 [19] J. S. Kavanaugh *et al.*, “Identification of extracellular DNA-binding proteins in the biofilm
431 matrix,” *mBio*, vol. 10, no. 3, May 2019, Accessed: Dec. 13, 2022. [Online]. Available:
432 <https://journals.asm.org/doi/10.1128/mBio.01137-19>
- 433 [20] T. Chavakis, K. Wiechmann, K. T. Preissner, and M. Herrmann, “*Staphylococcus aureus*
434 interactions with the endothelium. The role of bacterial ‘Secretable Expanded Repertoire
435 Adhesive Molecules’ (SERAM) in disturbing host defense systems,” *Thromb Haemost*, vol.
436 94, no. 2, pp. 278–285, Aug. 2005, doi: 10.1160/TH05-05-0306/ID/JR0306-11.
- 437 [21] T. Chavakis, K. T. Preissner, and M. Herrmann, “The anti-inflammatory activities of
438 *Staphylococcus aureus*,” *Trends Immunol*, vol. 28, no. 9, pp. 408–418, Sep. 2007, doi:
439 10.1016/J.IT.2007.07.002.
- 440 [22] M. Johnson, A. Cockayne, and J. A. Morrissey, “Iron-Regulated Biofilm Formation in
441 *Staphylococcus aureus* Newman Requires *ica* and the Secreted Protein Emp,” *Infect*
442 *Immun*, vol. 76, no. 4, p. 1756, Apr. 2008, doi: 10.1128/IAI.01635-07.
- 443 [23] K. M. Thompson, N. Abraham, and K. K. Jefferson, “*Staphylococcus aureus* extracellular
444 adherence protein contributes to biofilm formation in the presence of serum,” *FEMS*
445 *Microbiol Lett*, vol. 305, no. 2, p. 143, Apr. 2010, doi: 10.1111/J.1574-6968.2010.01918.X.
- 446 [24] D. A. C. Stapels *et al.*, “*Staphylococcus aureus* secretes a unique class of neutrophil serine
447 protease inhibitors,” *Proceedings of the National Academy of Sciences*, vol. 111, no. 36,
448 pp. 13187–13192, Sep. 2014, doi: 10.1073/pnas.1407616111.
- 449 [25] A. M. Palazzolo-Ballance *et al.*, “Neutrophil microbicides induce a pathogen survival
450 response in community-associated methicillin-resistant *Staphylococcus aureus*,” *J*
451 *Immunol*, vol. 180, no. 1, pp. 500–509, Jan. 2008, doi: 10.4049/JIMMUNOL.180.1.500.
- 452 [26] C. E. Heim, D. Vidlak, and T. Kielian, “Interleukin-10 production by myeloid-derived
453 suppressor cells contributes to bacterial persistence during *Staphylococcus aureus*
454 orthopedic biofilm infection,” *J Leukoc Biol*, vol. 98, no. 6, p. 1003, Dec. 2015, doi:
455 10.1189/JLB.4VMA0315-125RR.
- 456 [27] L. R. Thurlow *et al.*, “*Staphylococcus aureus* biofilms prevent macrophage phagocytosis
457 and attenuate inflammation in vivo.,” *J Immunol*, vol. 186, no. 11, pp. 6585–96, Jun.
458 2011, doi: 10.4049/jimmunol.1002794.
- 459 [28] C. F. Schierle, M. De La Garza, T. A. Mustoe, and R. D. Galiano, “Staphylococcal biofilms
460 impair wound healing by delaying reepithelialization in a murine cutaneous wound

- 461 model," *Wound Repair Regen*, vol. 17, no. 3, pp. 354–359, 2009, doi: 10.1111/J.1524-
462 475X.2009.00489.X.
- 463 [29] K. J. Yamada *et al.*, "Monocyte metabolic reprogramming promotes pro-inflammatory
464 activity and *Staphylococcus aureus* biofilm clearance," *PLoS Pathog*, vol. 16, no. 3, 2020,
465 doi: 10.1371/JOURNAL.PPAT.1008354.
- 466 [30] D. Vidlak and T. Kielian, "Infectious Dose Dictates the Host Response during
467 *Staphylococcus aureus* Orthopedic-Implant Biofilm Infection," *Infect Immun*, vol. 84, no.
468 7, pp. 1957–1965, 2016, doi: 10.1128/IAI.00117-16.
- 469 [31] R. M. Q. Shanks *et al.*, "Heparin stimulates *Staphylococcus aureus* biofilm formation.,"
470 *Infect Immun*, vol. 73, no. 8, pp. 4596–606, Aug. 2005, doi: 10.1128/IAI.73.8.4596-
471 4606.2005.
- 472 [32] C. Gil *et al.*, "Biofilm matrix exoproteins induce a protective immune response against
473 *Staphylococcus aureus* biofilm infection," *Infect Immun*, vol. 82, no. 3, pp. 1017–1029,
474 Mar. 2014, doi: 10.1128/IAI.01419-13/SUPPL_FILE/ZII999090534SO2.PDF.
- 475 [33] J. S. Kavanaugh *et al.*, "Identification of extracellular DNA-binding proteins in the biofilm
476 matrix," *mBio*, vol. 10, no. 3, May 2019, doi: 10.1128/MBIO.01137-
477 19/SUPPL_FILE/MBIO.01137-19-ST002.DOCX.
- 478 [34] J. Eisenbeis *et al.*, "The *Staphylococcus aureus* Extracellular Adherence Protein Eap Is a
479 DNA Binding Protein Capable of Blocking Neutrophil Extracellular Trap Formation," *Front*
480 *Cell Infect Microbiol*, vol. 8, Jul. 2018.
- 481 [35] M. Bhattacharya *et al.*, "*Staphylococcus aureus* biofilms release leukocidins to elicit
482 extracellular trap formation and evade neutrophil-mediated killing," *Proceedings of the*
483 *National Academy of Sciences*, Jun. 2018.
- 484 [36] V. Thammavongsa, H. K. Kim, D. Missiakas, and O. Schneewind, "Staphylococcal
485 manipulation of host immune responses.," *Nat Rev Microbiol*, vol. 13, no. 9, pp. 529–43,
486 2015.
- 487 [37] G. R. Pidwill, J. F. Gibson, J. Cole, S. A. Renshaw, and S. J. Foster, "The Role of
488 Macrophages in *Staphylococcus aureus* Infection," *Front Immunol*, vol. 11, p. 620339,
489 Jan. 2021, doi: 10.3389/FIMMU.2020.620339/BIBTEX.
- 490 [38] L. Shipman, "Neutrophils: Sizing up pathogens," Jan. 01, 2014, *Nature Publishing Group*.
491 doi: 10.1038/nri3756.
- 492 [39] C. E. Heim, D. Vidlak, T. D. Scherr, C. W. Hartman, K. L. Garvin, and T. Kielian, "Interleukin-
493 12 promotes myeloid-derived suppressor cell (MDSC) recruitment and bacterial
494 persistence during *S. aureus* orthopedic implant infection," *J Immunol*, vol. 194, no. 8, p.
495 3861, Apr. 2015, doi: 10.4049/JIMMUNOL.1402689.
- 496 [40] M. L. Hanke, C. E. Heim, A. Angle, S. D. Sanderson, and T. Kielian, "Targeting macrophage
497 activation for the prevention and treatment of *Staphylococcus aureus* biofilm
498 infections.," *J Immunol*, vol. 190, no. 5, pp. 2159–68, Mar. 2013, doi:
499 10.4049/jimmunol.1202348.
- 500 [41] A. L. Aldrich, C. M. Horn, C. E. Heim, L. E. Korshoj, and T. Kielian, "Transcriptional
501 Diversity and Niche-Specific Distribution of Leukocyte Populations during *Staphylococcus*
502 *aureus* Craniotomy-Associated Biofilm Infection," *J Immunol*, vol. 206, no. 4, pp. 751–
503 765, Feb. 2021, doi: 10.4049/JIMMUNOL.2001042.

- 504 [42] C. E. Heim *et al.*, “Myeloid-derived suppressor cells (MDSCs) contribute to *S. aureus*
505 orthopedic biofilm infection,” *J Immunol*, vol. 192, no. 8, p. 3778, Apr. 2014, doi:
506 10.4049/JIMMUNOL.1303408.
- 507 [43] D. Kretschmer *et al.*, “*Staphylococcus aureus* Depends on Eap Proteins for Preventing
508 Degradation of Its Phenol-Soluble Modulins by Neutrophil Serine Proteases,” *Front*
509 *Immunol*, vol. 12, p. 3605, Sep. 2021, doi: 10.3389/FIMMU.2021.701093/BIBTEX.
- 510 [44] S. S. Dastgheyb *et al.*, “Role of phenol-soluble modulins in formation of *Staphylococcus*
511 *aureus* biofilms in synovial fluid,” *Infect Immun*, vol. 83, no. 7, pp. 2966–2975, 2015, doi:
512 10.1128/IAI.00394-15/ASSET/F34A1813-260C-4026-9A4D-
513 E77CFF1B8ACE/ASSETS/GRAPHIC/ZII9990913060007.JPEG.
- 514 [45] K. Schwartz, A. K. Syed, R. E. Stephenson, A. H. Rickard, and B. R. Boles, “Functional
515 amyloids composed of phenol soluble modulins stabilize *Staphylococcus aureus*
516 biofilms,” *PLoS Pathog*, vol. 8, no. 6, p. e1002744, Jan. 2012, doi:
517 10.1371/journal.ppat.1002744.
- 518 [46] M. Bhattacharya *et al.*, “Leukocidins and the nuclease Nuc prevent neutrophil mediated
519 killing of *Staphylococcus aureus* biofilms,” *Infect Immun*, Jul. 2020.
- 520 [47] T. J. Scriba, S. Sierro, E. L. Brown, R. E. Phillips, A. K. Sewell, and R. C. Massey, “The
521 *Staphylococcus aureus* eap protein activates expression of proinflammatory cytokines,”
522 *Infect Immun*, vol. 76, no. 5, pp. 2164–2168, May 2008, doi: 10.1128/IAI.01699-
523 07/ASSET/13B49694-7E28-4289-BF2F-
524 F23A73DB5E2A/ASSETS/GRAPHIC/ZII0050872860005.JPEG.
- 525 [48] T. D. Scherr *et al.*, “*Staphylococcus aureus* Biofilms Induce Macrophage Dysfunction
526 Through Leukocidin AB and Alpha-Toxin,” *mBio*, vol. 6, no. 4, pp. e01021-15, Aug. 2015,
527 doi: 10.1128/mBio.01021-15.
- 528 [49] A. Hagggar, O. Shannon, A. Norrby-Teglund, and J. I. Flock, “Dual effects of extracellular
529 adherence protein from *Staphylococcus aureus* on peripheral blood mononuclear cells,” *J*
530 *Infect Dis*, vol. 192, no. 2, pp. 210–217, Jul. 2005, doi: 10.1086/430948.
- 531 [50] A. Hagggar, J. I. Flock, and A. Norrby-Teglund, “Extracellular adherence protein (Eap) from
532 *Staphylococcus aureus* does not function as a superantigen,” *Clinical Microbiology and*
533 *Infection*, vol. 16, no. 8, pp. 1155–1158, Aug. 2010, doi: 10.1111/j.1469-
534 0691.2009.03058.x.
- 535 [51] A. J. Seidman and F. Limaiem, “Synovial Fluid Analysis,” *StatPearls*, May 2023, Accessed:
536 Apr. 14, 2024. [Online]. Available: <https://www.ncbi.nlm.nih.gov/books/NBK537114/>
- 537 [52] P. Stoodley *et al.*, “Direct demonstration of viable *Staphylococcus aureus* biofilms in an
538 infected total joint arthroplasty. A case report,” *J Bone Joint Surg Am*, vol. 90, no. 8, pp.
539 1751–8, Aug. 2008, doi: 10.2106/JBJS.G.00838.
- 540 [53] S. J. McConoughey *et al.*, “Biofilms in periprosthetic orthopedic infections,” *Future*
541 *Microbiol*, vol. 9, no. 8, pp. 987–1007, Aug. 2014, doi: 10.2217/fmb.14.64.
- 542 [54] M. J. Pestrak *et al.*, “Investigation of synovial fluid induced *Staphylococcus aureus*
543 aggregate development and its impact on surface attachment and biofilm formation,”
544 *PLoS One*, vol. 15, no. 4, Apr. 2020, Accessed: Jun. 14, 2023. [Online]. Available:
545 /pmc/articles/PMC7164621/

- 546 [55] A. Staats *et al.*, “Synovial Fluid-Induced Aggregation Occurs across *Staphylococcus aureus*
547 Clinical Isolates and is Mechanistically Independent of Attached Biofilm Formation,”
548 *Microbiol Spectr*, vol. 9, no. 2, Oct. 2021, doi: 10.1128/SPECTRUM.00267-21.
- 549 [56] M. R. Kiedrowski *et al.*, “Nuclease modulates biofilm formation in community-associated
550 methicillin-resistant *Staphylococcus aureus*,” *PLoS One*, vol. 6, no. 11, p. e26714, Jan.
551 2011, doi: 10.1371/journal.pone.0026714.
552

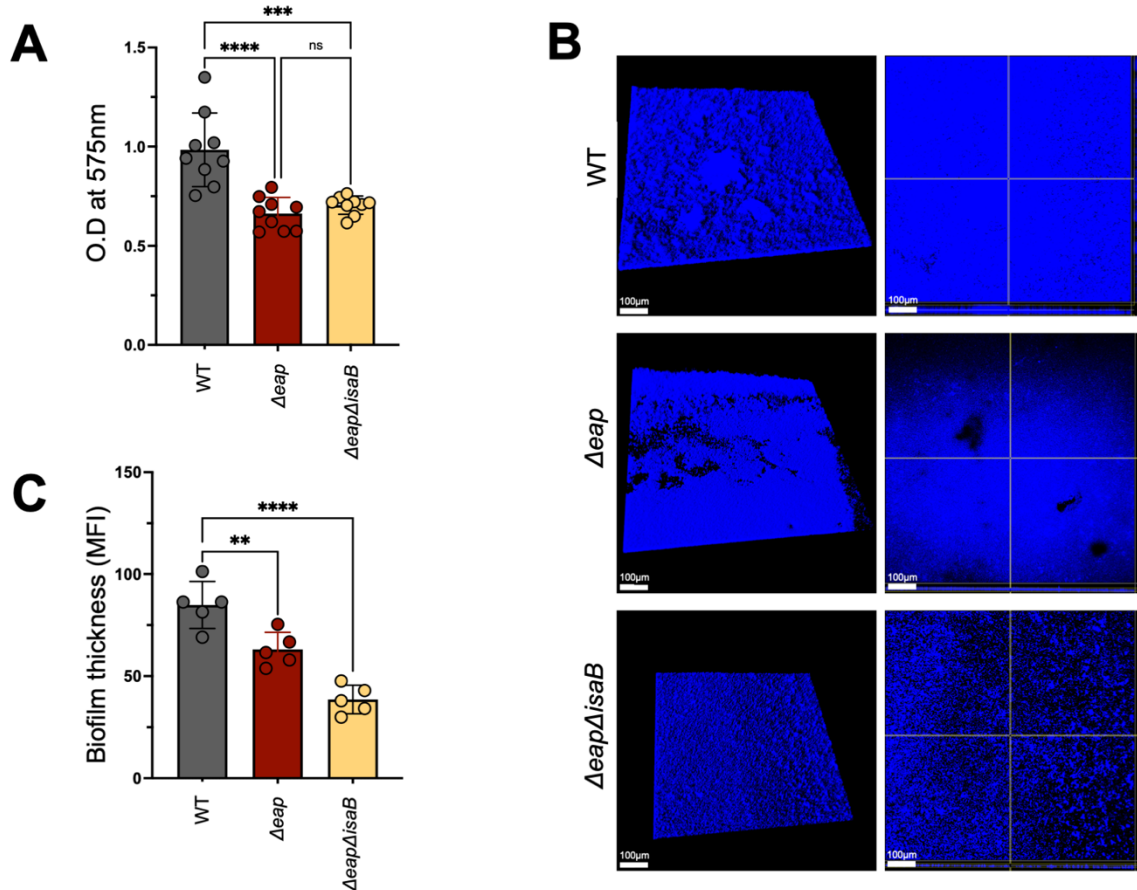


Figure 1. Eap proteins contribute to biofilm biomass. Crystal violet assay measuring biomass of WT, Δeap and $\Delta eap\Delta isaB$ biofilms grown overnight in 96-well plates. Crystal violet staining was measured as O.D. at 575nm using previously established methods (A). 3-dimensional confocal microscopy images of WT, Δeap and $\Delta eap\Delta isaB$ biofilms grown similarly to A, in 8-well chamber slides. Bacteria were stained with Hoechst Blue 33342 and images were captured at 400X magnification (left). Images of sections were taken close to the bottom of the biofilm for each strain (right) (B). Volume quantification of biofilms grown as described for B (C). Data represent 3 independent experiments performed in triplicate. Multiple comparisons were made with one-way analysis of variance and Tukey's post hoc test. ****, $P < 0.0001$; ***, $P < 0.001$; **, $P < 0.01$; ns, not significant. Images were taken using Imaris software. MFI calculations were done using ImageJ software.

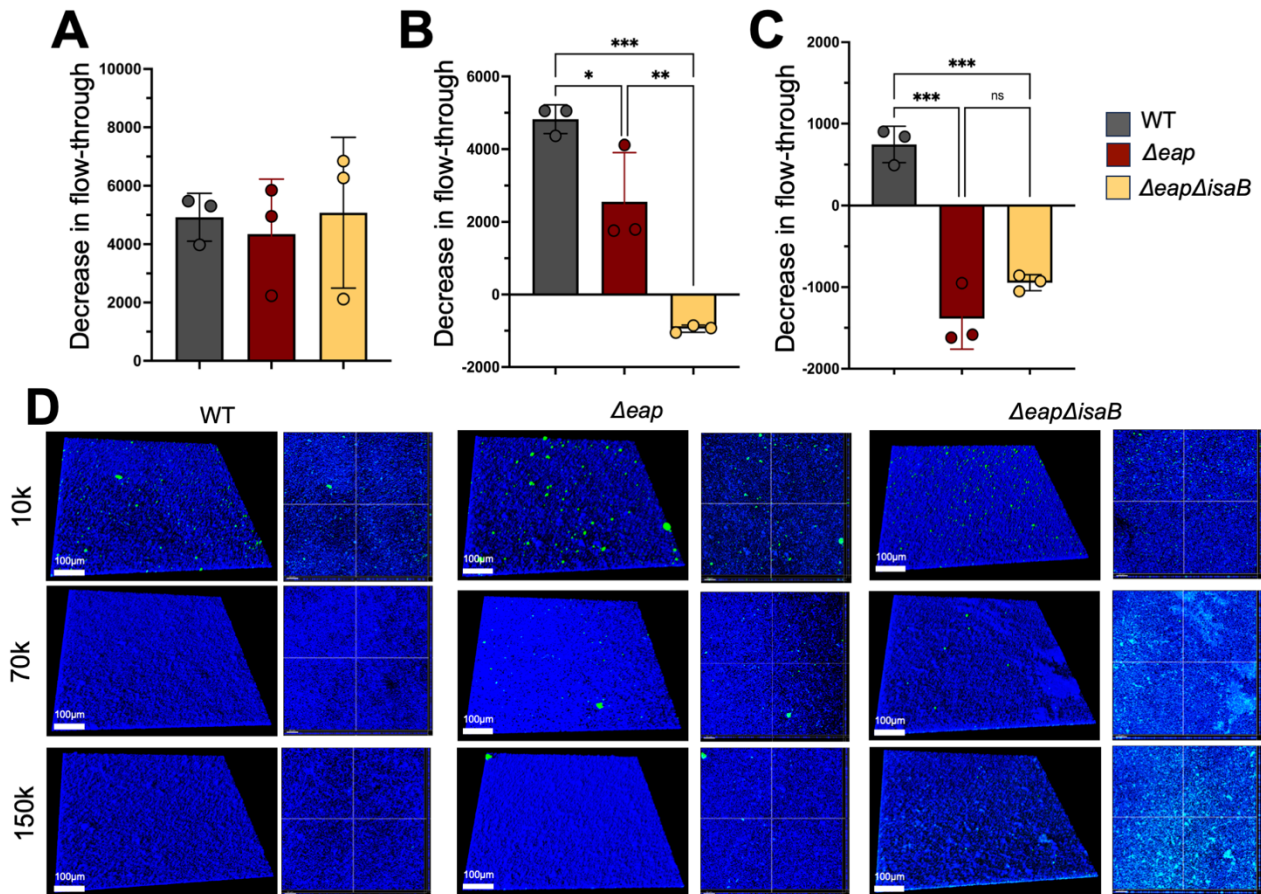


Figure 2. Eap proteins reduce biofilm porosity. Flow through of 10, 70 and 150kD FITC-labelled dextran from WT, Δeap and $\Delta eap\Delta isaB$ biofilms grown on 0.45 μ m PVDF membranes. Results are calculated in relative fluorescence units as compared to control biofilms lacking dextran (A-C). Representative 3D confocal images of biofilms grown in 6-well ibidi chamber slides after incubation with FITC-labelled dextran of respective molecular weights (D). Multiple comparisons were made with one-way analysis of variance and Tukey's post hoc test. ***, P < 0.001; **, P < 0.01; *, P < 0.1; ns, not significant. Images were taken using Imaris software.

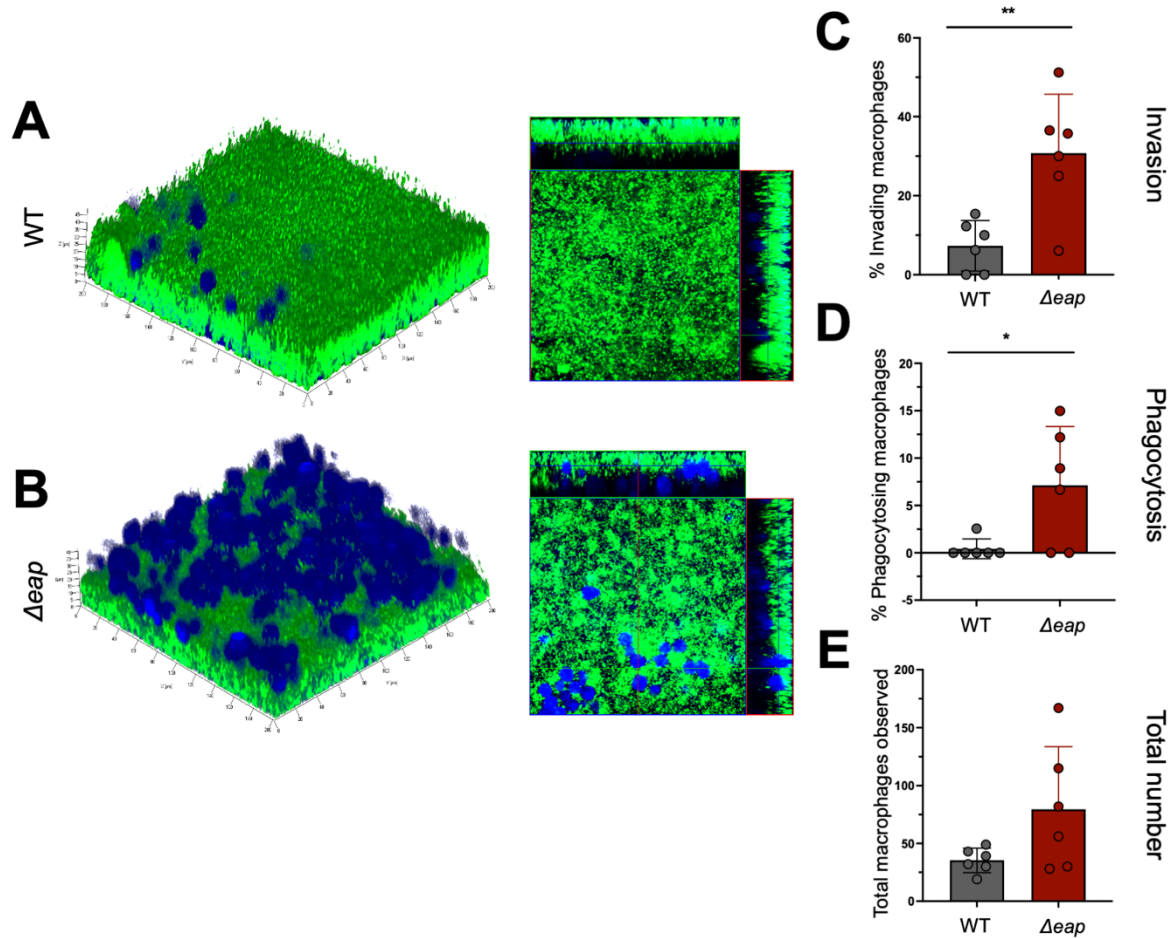


Figure 3. Eap proteins protect biofilms against macrophages. Representative 3D confocal images of green fluorescent protein (GFP)-labelled WT (A) or Δeap (B) biofilms incubated with Cell Tracker Blue labelled macrophages for 4-6 hours (left). Cross sectional images from biofilms shown on left (right). Quantification macrophages invading WT or Δeap biofilms (C), phagocytosing bacteria (D) and total numbers observed (E). Student *t* tests were performed for pairwise comparisons.**, P value = 0.0055; *, P value= 0.0261.

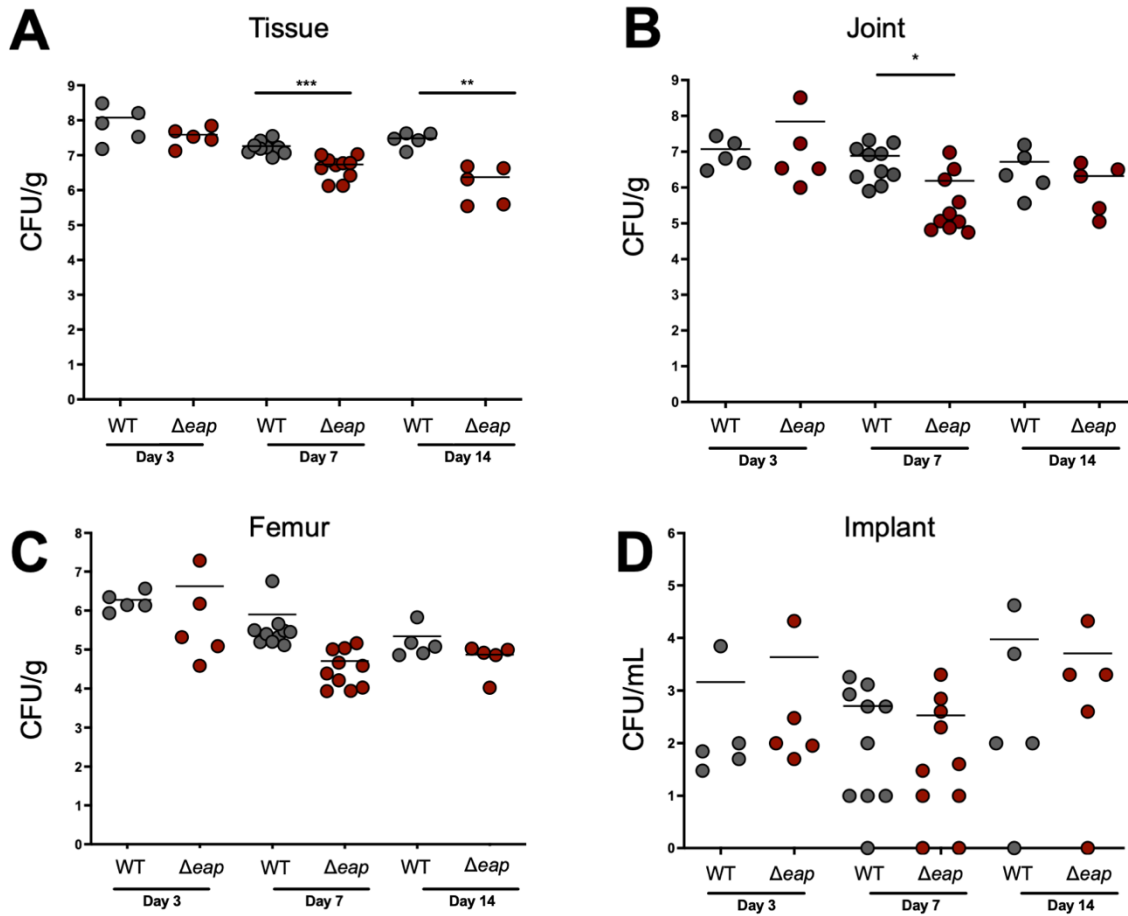


Figure 4. Eap proteins promote bacterial survival during prosthetic joint infection. Bacterial burdens were quantified in C57BL/6 mice infected with WT or Δeap *S. aureus* at the indicated time points post-infection in the soft tissue surrounding the knee (A), joint (B), femur (C), and sonicated titanium implant (D)(n=5-10 mice/group). Student's test was performed for pair-wise comparison.*** P value= 0.0001, ** P value= 0.0061 *P value= 0.0239

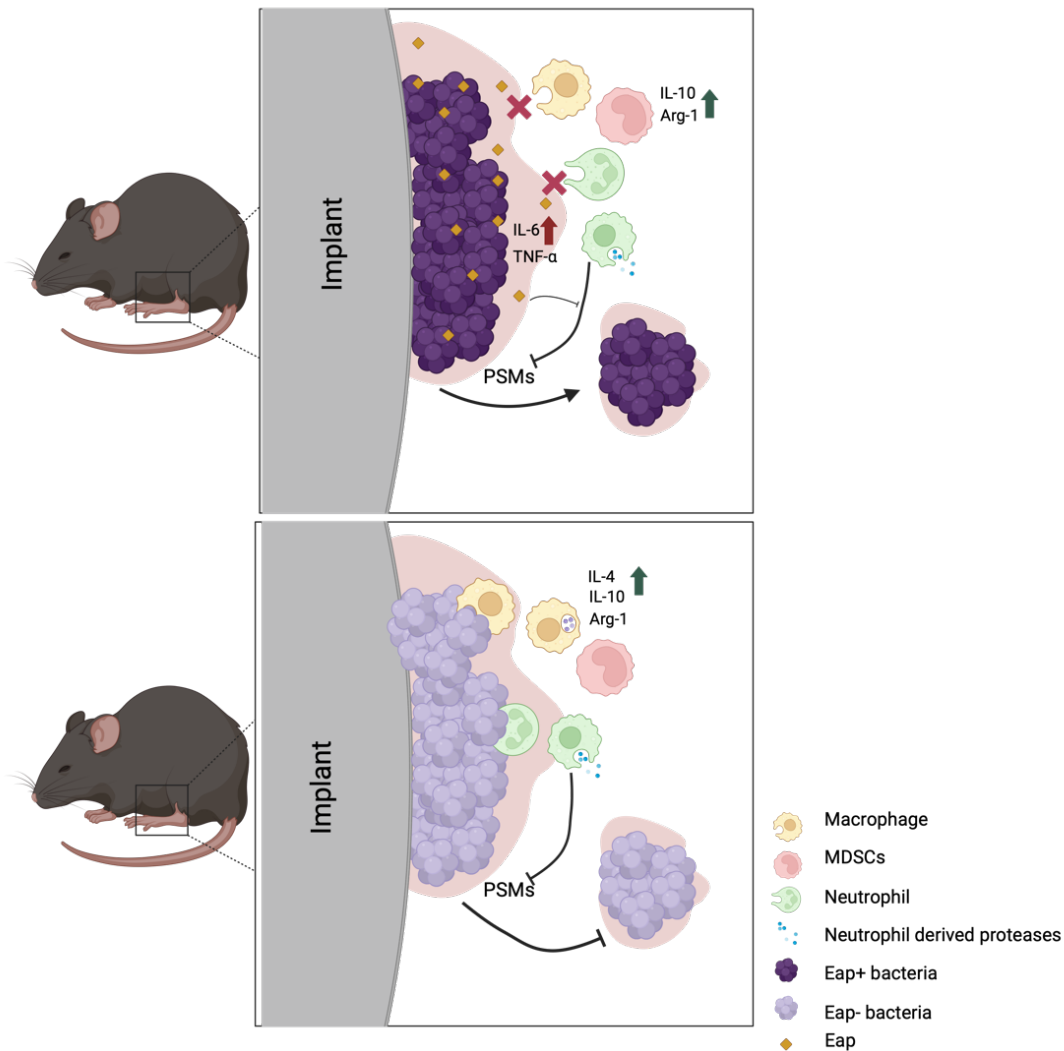


Figure 5. Summary and hypotheses based on current findings and previous literature.

Expression of Eap protects biofilms from macrophage invasion and phagocytosis and, to a lesser extent, neutrophils. Proinflammatory signatures associated with Eap expression are likely dampened by the anti-inflammatory macrophage response to biofilms. Eap proteins prevent protease-mediated degradation of phenol soluble modulins (PSMs), which allows for subpopulations of the community to disperse and spread (A). In the absence of Eap, phagocytes gain some entry into the biofilm and likely phagocytose and kill bacteria. Proteases released from neutrophils degrade PSMs and prevent dispersion allowing the immune response to continue clearance of the biofilm infection. Inflammation is reduced in the presence of anti-inflammatory signatures generated from biofilm-exposed macrophages (B).